Use of Nano Seed Crystals to Control Peroxide Morphology in a Nonaqueous Li-O_2 Battery

Ganapathy, Swapna; Li, Zhaolong; Anastasaki, Maria S.; Basak, Shibabrata; Miao, Xue Fei; Goubitz, Kees; Zandbergen, Henny W.; Mulder, Fokko M.; Wagemaker, Marnix

DOI
10.1021/acs.jpcc.6b04732

Publication date
2016

Document Version
Accepted author manuscript

Published in
The Journal of Physical Chemistry C

Supporting information

The Use of Nano Seed Crystals to Control Peroxide Morphology in a Non-Aqueous Li-O_2 Battery

Swapna Ganapathy, Zhaolong Li, Maria S. Anastasaki, Shibabrata Basak, Xue-Fei Miao, Kees Goubitz, Henny W. Zandbergen, Fokko M. Mulder and Marnix Wagemaker*

Materials and Methods

Nickel Oxide synthesis: The rhombohedral phase of NiO was obtained by heating nickel carbonate basic hydrate (99.9% trace metal basis, Sigma Aldrich) to 1200 ^{o}C for 24 h under ambient air after which it was slowly cooled. The obtained product was tested with X-ray diffraction (XRD) and the resulting pattern was fit with the General Structure Analysis System (GSAS) program[1] using the Rietveld method to verify the phase of the material (Figure S1). This material was further nanosized by ball milling. Five cycles, each comprising a 5-minute milling process at 500 rpm followed by a 20-minute rest period was performed. Further XRD and TEM analysis and refinement showed that the resultant NiO nanoparticles had an average domain size of 5-10 nm.

Electrode preparation and Electrochemistry: Gas diffusion electrodes (cathodes) were prepared, with Activated Carbon (AC, Kuraray Chemical) and with Activated Carbon containing NiO nanoparticles (with AC:NiO weight ratios of 95:5 (AC-NiO-1) and 33.3:66.6 (AC-NiO-2) respectively) and a lithiated Nafion®[2, 3] binder in N-Methyl-2-pyrrolidone (NMP, Aldrich).The mixture of AC-NiO was ball milled at a low speed of 100 rpm to ensure proper contact between AC and NiO. Slurries of AC and the AC-NiO mixtures and binder (90:10 by weight) were cast on carbon paper (Spectracarb 2050a). These cathodes were further dried under vacuum at 100 °C for 24 h to remove all traces of surface adsorbed water, upon which discs 11 and 19 mm in diameter were punched out. The final mass of AC/AC-NiO-1 on carbon paper was ~ 2 – 3 mg/cm^2 while that of AC-NiO-2 on carbon paper was ~4 – 5 mg/cm^2. The electrolyte used was a solution of 1M lithium bis(trifluoromethanesulfonyl)imide (LiTFSI, Aldrich) dissolved in dried and distilled

tetraethylene glycol dimethyl ether (TEGDME, <5 ppm H_2O, Aldrich). Batteries comprising a cathode, glass microfiber separator (Whatman) soaked with electrolyte and a Li-metal anode were assembled in a glove box (Argon, O_2 and H_2O < 0.1 ppm) in our home-built cells for non-aqueous Li-O_2 batteries, as well as in our special cells for *operando* X-ray diffraction.[4] Once connected to O_2 (Linde, 99.995%) the cell was allowed to equilibrate for 2 – 6 h under an O_2 pressure of 1.2 bar. Galvanostatic (dis)charge cycles were performed using a MACCOR 5300 battery cycler.

XRD measurements: X-ray diffraction measurements were performed during the operation of a Li-O_2 cell using a PANalytical X'Pert Pro PW3040/60 diffractometer with Cu Kα radiation operating at 45kV and 40 mA in an angular 2θ range of 31 – 66°. Each scan was 67 minutes long. Rietveld refinement of the diffraction data was performed using the aforementioned GSAS program. Several variables including the lattice parameters, peak broadening and anisotropy (if present) and occupancies were fit, assuming the vibrational spectrum remained constant. Peaks arising from the aluminum mesh and carbon paper were excluded from the fits to enable a more accurate fit of the zero-position of the diffraction patterns.

TEM measurements: For preparing the TEM samples, the NiO sample was ultrasonicated in acetone for 30 minutes before dispersing on a standard TEM Cu-grid. TEM measurements were carried out in a Cs corrected TITAN microscope operating at 300 KV.

SEM measurements: Morphology of the discharged cathodes were characterized using Hitachi 4800S scanning electron microscope with cold FEG electron gun operated at 5 kV. SEM_EDX measurements were performed on a FEI Nova NanoSEM 450 equipped with EDAX TEAM operating at 15 kV.

Theoretical calculations: First-principle calculations were performed using the Heyd−Scuseria−Ernzerhof (HSE)[5, 6] hybrid functional as applied in the Vienna Ab-Initio simulation package (VASP)[7] with the projector augmented wave (PAW) method,[8] because of its demonstrated ability to describe the electronic properties of Li_2O_2.[9] The energy cut-off was set to 600 eV, along with convergence criteria of 10^{-4} eV/formula unit for ionic relaxation.

In order to determine the excess energy that would occur as a result of an interface between periodic regions of NiO and Li_2O_2 the following protocol was employed. Two slabs with the in-plane interfacial dimensions of 2.967 Å × 2.967 Å and 3.070 Å × 3.070 Å were constructed consisting of periodic regions of (0 0 1) NiO and (0 0 1) Li_2O_2. The relaxed slab lengths of 29.9 Å (2.967 Å × 2.967 Å) and 30.5 Å (3.070 Å × 3.070 Å) were determined in the direction perpendicular to the interface. Additionally ionic relaxation was performed such that the total energy convergence was below 10^{-4} eV. In order to avoid contributions from elastic energy which would arise as a result of enforced strain the following method was employed. For the cells representing the bulk contributions of NiO and Li_2O_2, the cell parameters in the plane of the interface *i.e.* a/b parameters were fixed to the same values as that for the interface used in the slab (2.967 or 3.070 Å), while only the cell parameter in the direction perpendicular to the interface was relaxed. As a result when the bulk energy was subtracted from the interface slab energy, it was ensured that the energy arising as a result of elastic strain was also subtracted. The interface energy was determined to be 0.156 eV/Å^2 for the 2.967 Å × 2.967 Å interface and 0.22 eV/Å^2 for the 3.070 Å × 3.070 Å interface respectively.

Li_2O_2 titration: We followed the protocol for Li_2O_2 titration that has been described in detail the article published by McCloskey and co-workers.[10] Cathodes were extracted from the battery in the argon filled glove box, where they were transferred into glass vials and the tops were closed

off with a tightly wrapped parafilm layer. These sealed bottles were taken out of the glove box, where they were injected with 2 – 3 mL of ultrapure water using a syringe. After shaking vigorously, the contents of the bottle were transferred to a 50 mL Erlenmeyer flask, where the base formed was titrated against a standardized 0.005M HCl (Sigma-Aldrich) solution using a drop of phenolphthalein (Sigma-Aldrich) in alcohol as the end-point indicator. After this, three reagents were added in quick succession. First, 1 mL of a 2 wt% KI (≥99.5 %, Sigma-Aldrich) solution in H_2O, followed by 1 mL of 3.5 M H_2SO_4 solution, followed finally by 50 μL of a molybdate-based catalyst solution. The molybdate-based catalyst solution was prepared by combining 1 g of ammonium molybdate (Sigma-Aldrich) with 10 mL of 6N NH_4OH (Sigma-Aldrich), to which 3 g of ammonium nitrate (≥98 %, Sigma-Aldrich) was added after which the mixture was diluted to 50 mL using ultrapure H_2O. Upon addition of these reagents, the solution in the flask turns yellow due to the formation of I_2 which is subsequently titrated against a standardized solution of 0.01 N $Na_2S_2O_3$ (Sigma-Aldrich) to a faint straw color. At this point ~0.5 mL a 1% starch solution (Sigma-Aldrich) is added as an end-point indicator turning the solution a deep blue, and the solution is further titrated until the solution turns colorless.

Iodometric titrations performed on commercially purchased Li_2O_2 powder (Sigma-Aldrich, 90% purity) with 1 mg of Li_2O_2 dissolved in 3 mL of ultrapure water yielded a Li_2O_2 purity of 83.1 ± 1.5% over three titrations, which gives an approximate percentage error of 6 - 8 % per titration. The percentage yield of Li_2O_2 was determined by dividing the amount of Li_2O_2 titrated (A), by the amount of Li_2O_2 that would be expected if a 2.0 e^- per Li_2O_2 reaction occurred during discharge (B). For a 1 mAh discharge capacity, theoretically 18.65 μmols of Li_2O_2 would be expected to be formed.

Description of the specific capacity: Given the variety in dimension, coating thicknesses, carbon/active material loading, porosity, and actual surface areas reported for gas diffusion electrodes in literature, a realistic comparison of currents used and specific capacities in terms of mAh/g_{carbon} or mAh/cm^2 becomes difficult. Given what is now known about the formation of peroxide and how its formation is restricted to the surface of the gas diffusion electrode as well as to allow a consistent comparison between capacities obtained with our own cathodes, with and without NiO seed crystals, we have reported all our results in terms of specific capacities per cm^2 (mAh/cm^2).

Note on the total surface area of AC-NiO-1 and AC-NiO-2: The Activated Carbon (YP-50F, Kurary Chemicals, Japan) used for our electrodes has a high total surface area of 1500-1800 m^2/g. This corresponds to a roughly estimated 2 nm particle size. The NiO particles are on average, 2 to 5 times larger than the AC particles so the AC-NiO-2 electrodes, which contain 30% NiO have a lower surface area than the AC-NiO-1 electrodes.

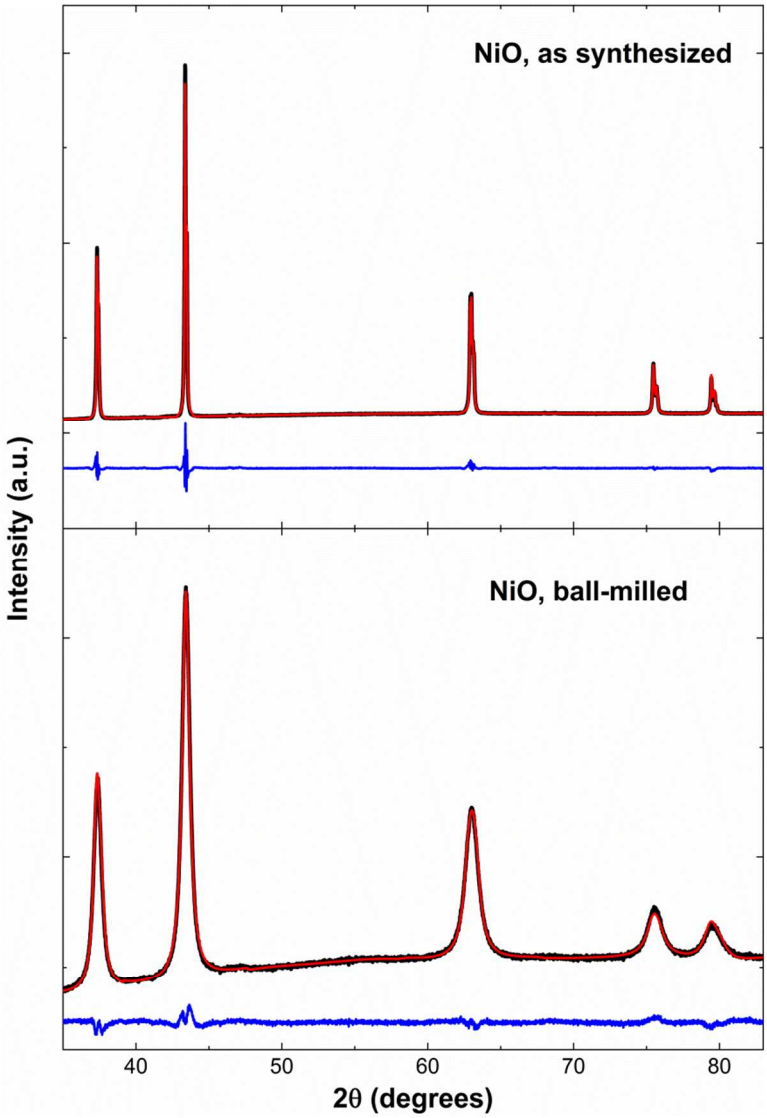

Figure S1 XRD patterns with corresponding Rietveld refinement of as synthesized and ball milled NiO. The black line represents the pattern as measured, the red line the fit and the blue line the difference.

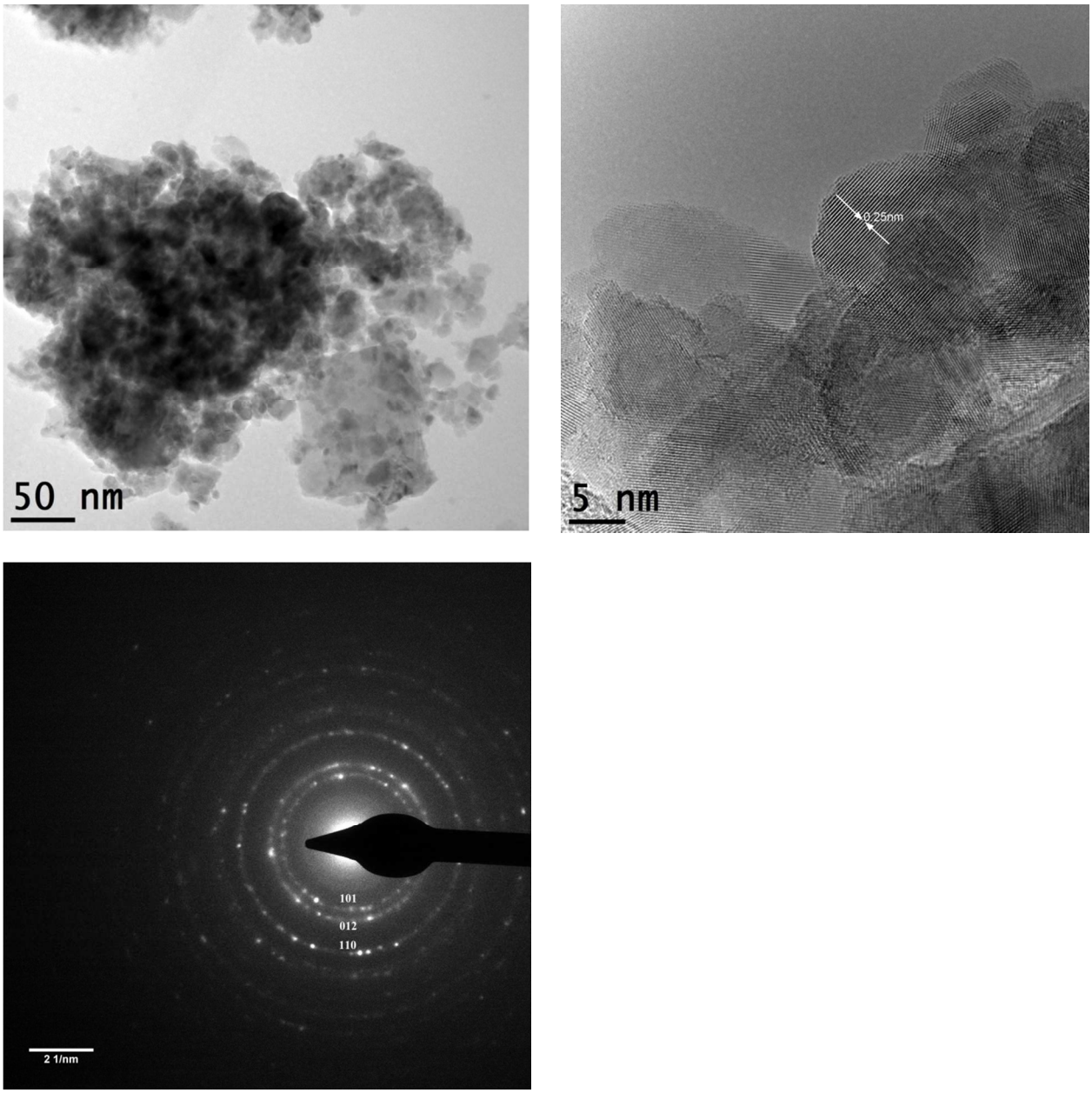

Figure S2 TEM image of the agglomerate of NiO nanoparticles, the hexagonal {10-10}/{1-100} d-spacing indicated, and the SAED patterns indicating several hexagonal NiO indexed rings.

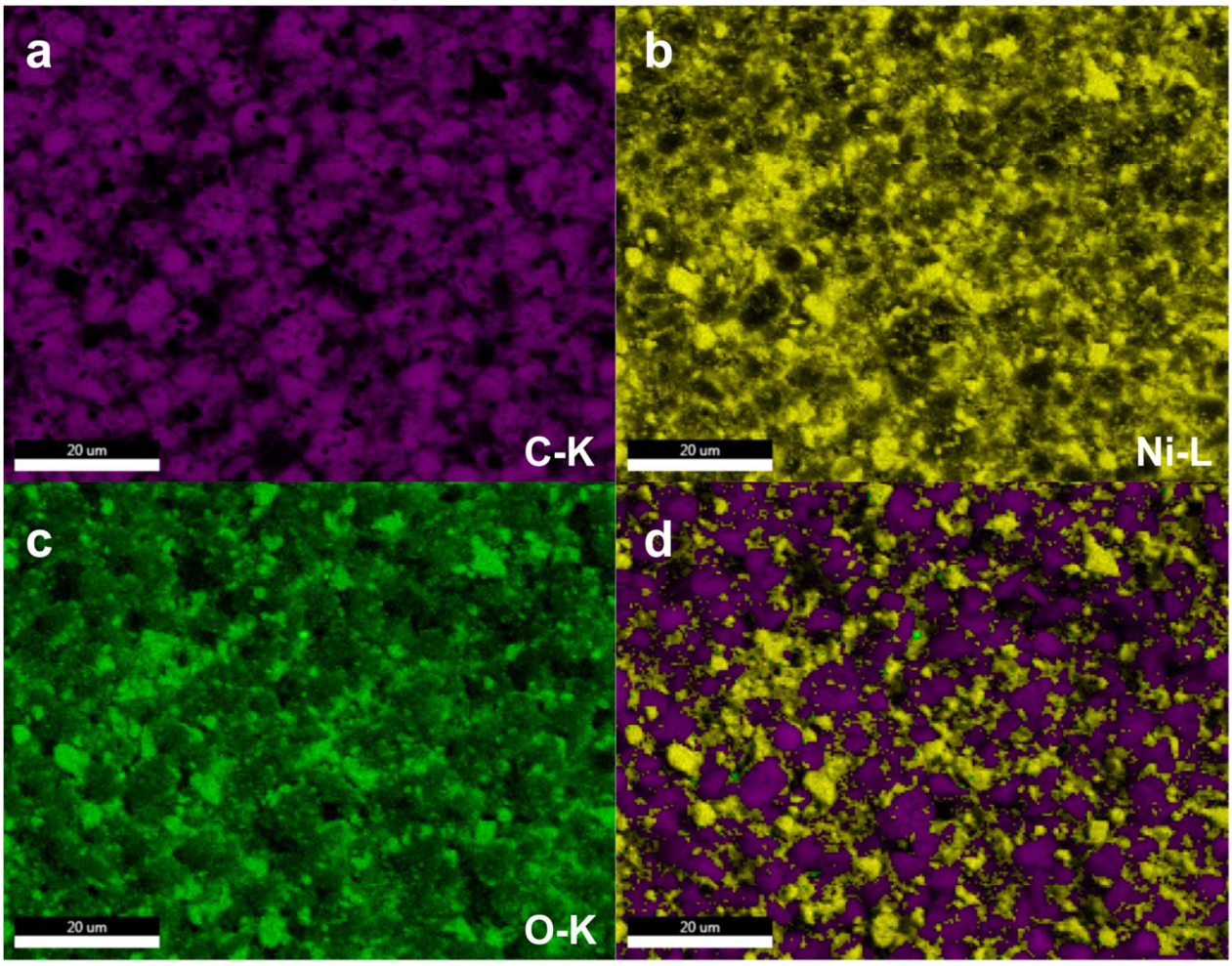

Figure S3 SEM-EDX elemental mapping of a pristine AC-NiO-2 electrode showing maps of (a) C (b) Ni (c) O and (d) overlay with purple = C; yellow = Ni; and green = O; The scale bar corresponds to 20 μm.

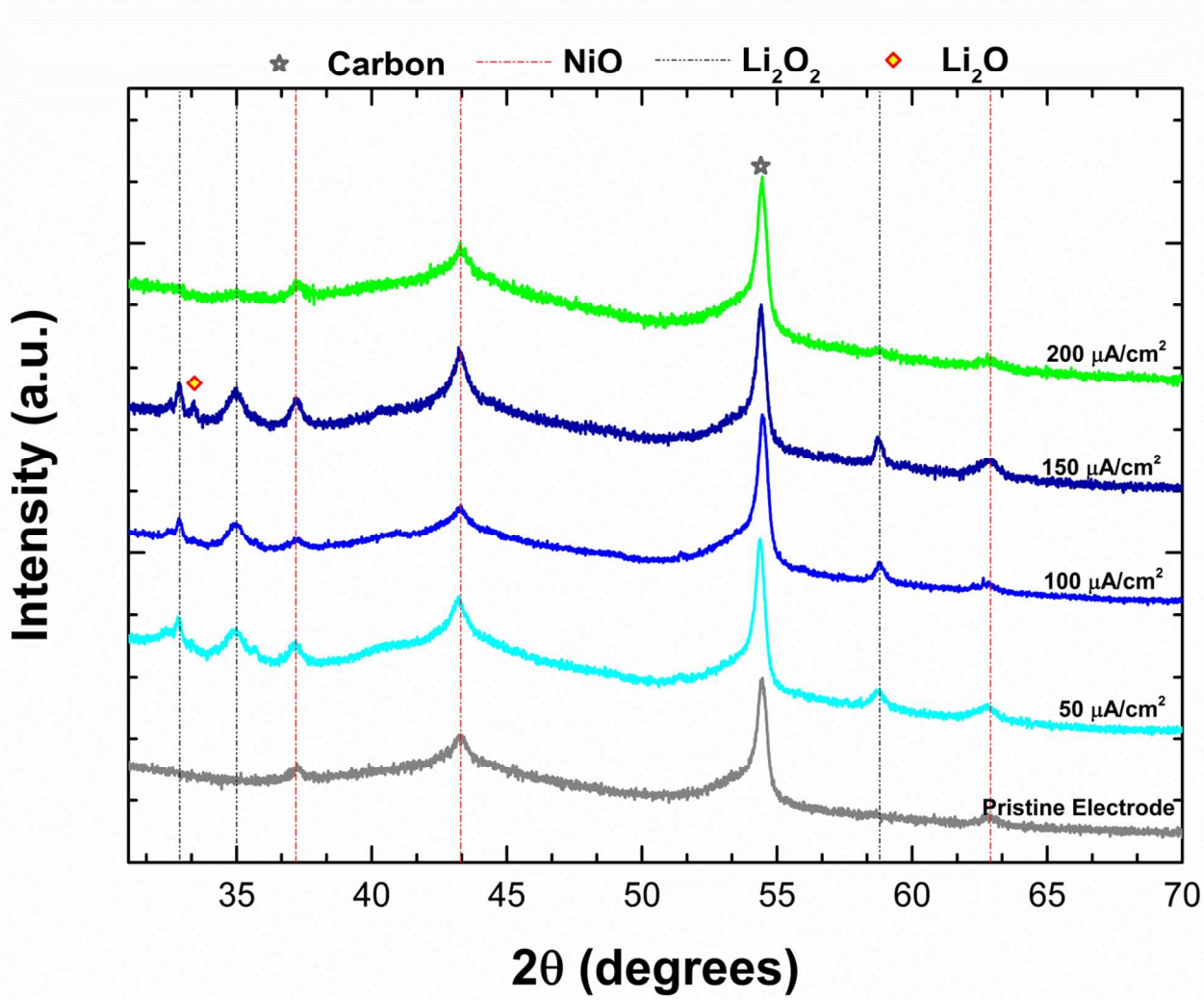

Figure S4 Full XRD patterns of AC-NiO-1 electrodes completely discharged at different current densities.

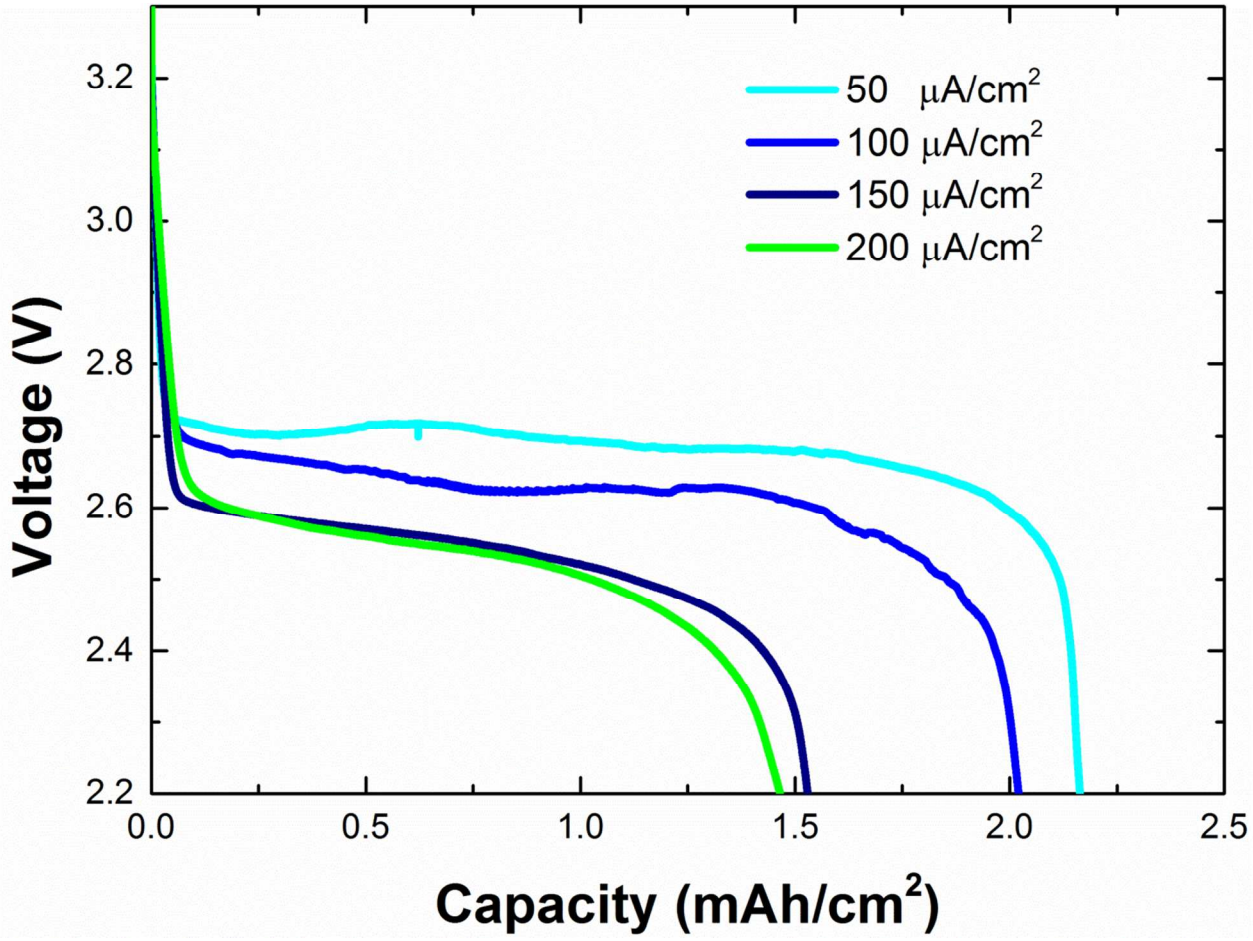

Figure S5 Galvanostatic discharge profiles of the AC electrodes in a Li-O_2 cell at current densities of 50 – 200 μA/ cm^2 (lower voltage cut-off set at 2.2 V).

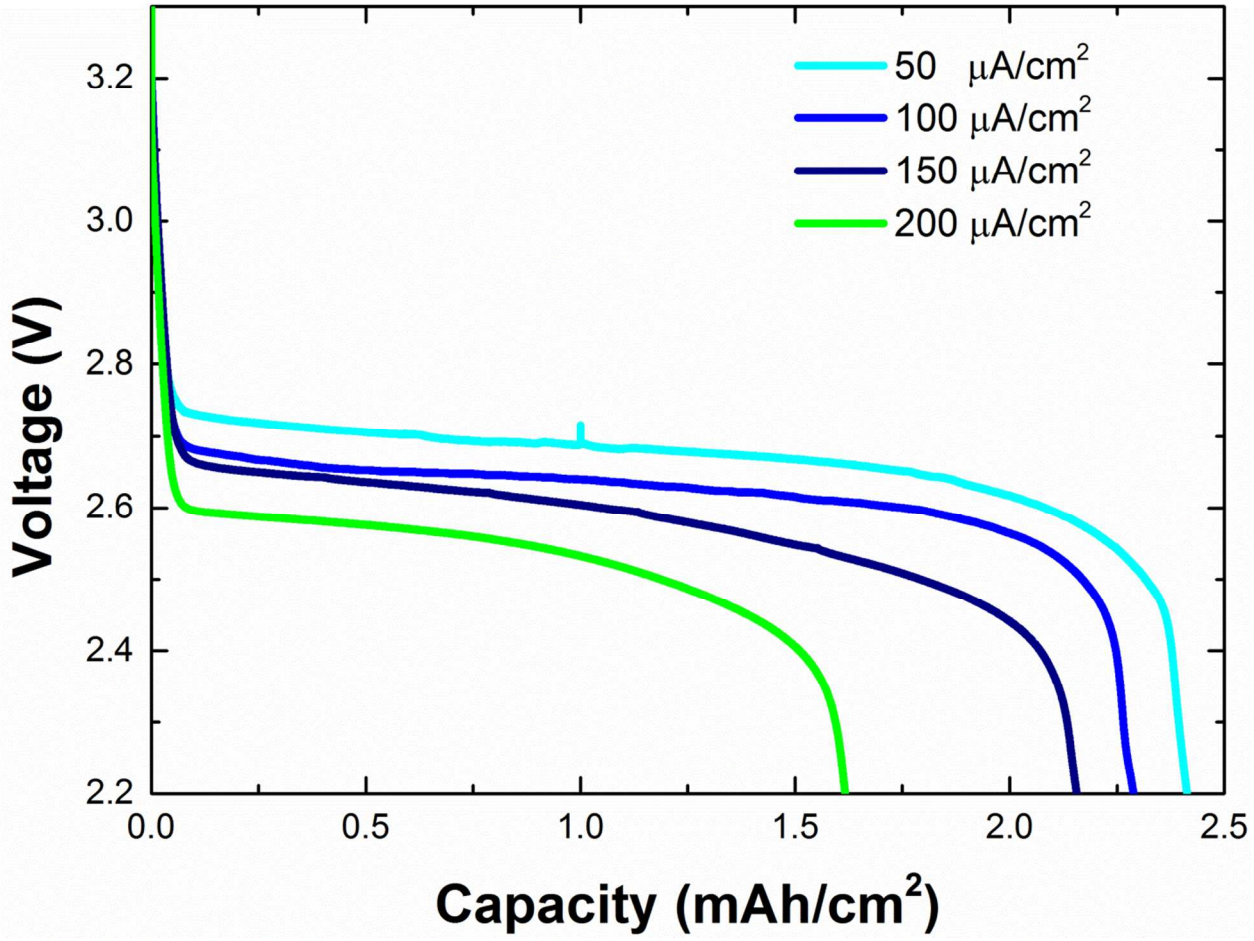

Figure S6 Galvanostatic discharge profiles of the AC-NiO-1 electrodes in a Li-O_2 cell at current densities of 50 – 200 μA/ cm^2 (lower voltage cut-off set at 2.2 V).

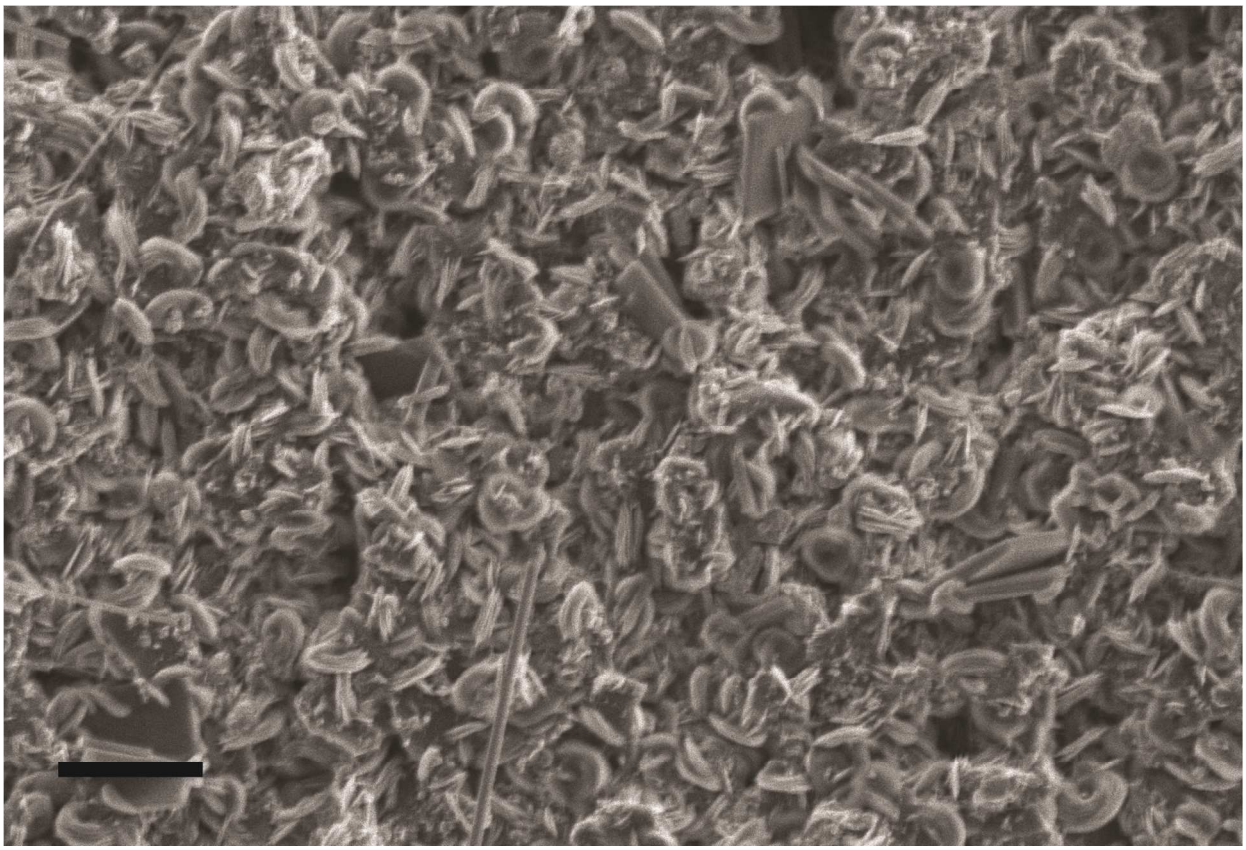

Figure S7 Scanning electron microscopy (SEM) images recorded at the end of discharge with a current density of 50 μA/cm^2 of the AC-NiO-2 cathode. The scale bar represents 5 μm.

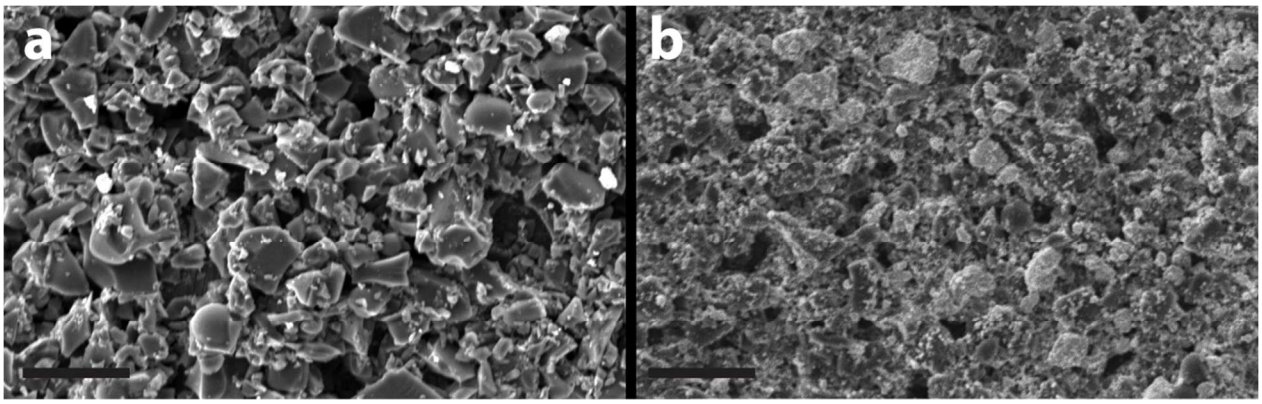

Figure S8 Scanning electron microscopy (SEM) images recorded of the pristine (a) AC-NiO-1 and (b) AC-NiO-2 cathodes. The scale bar represents 10 μm.

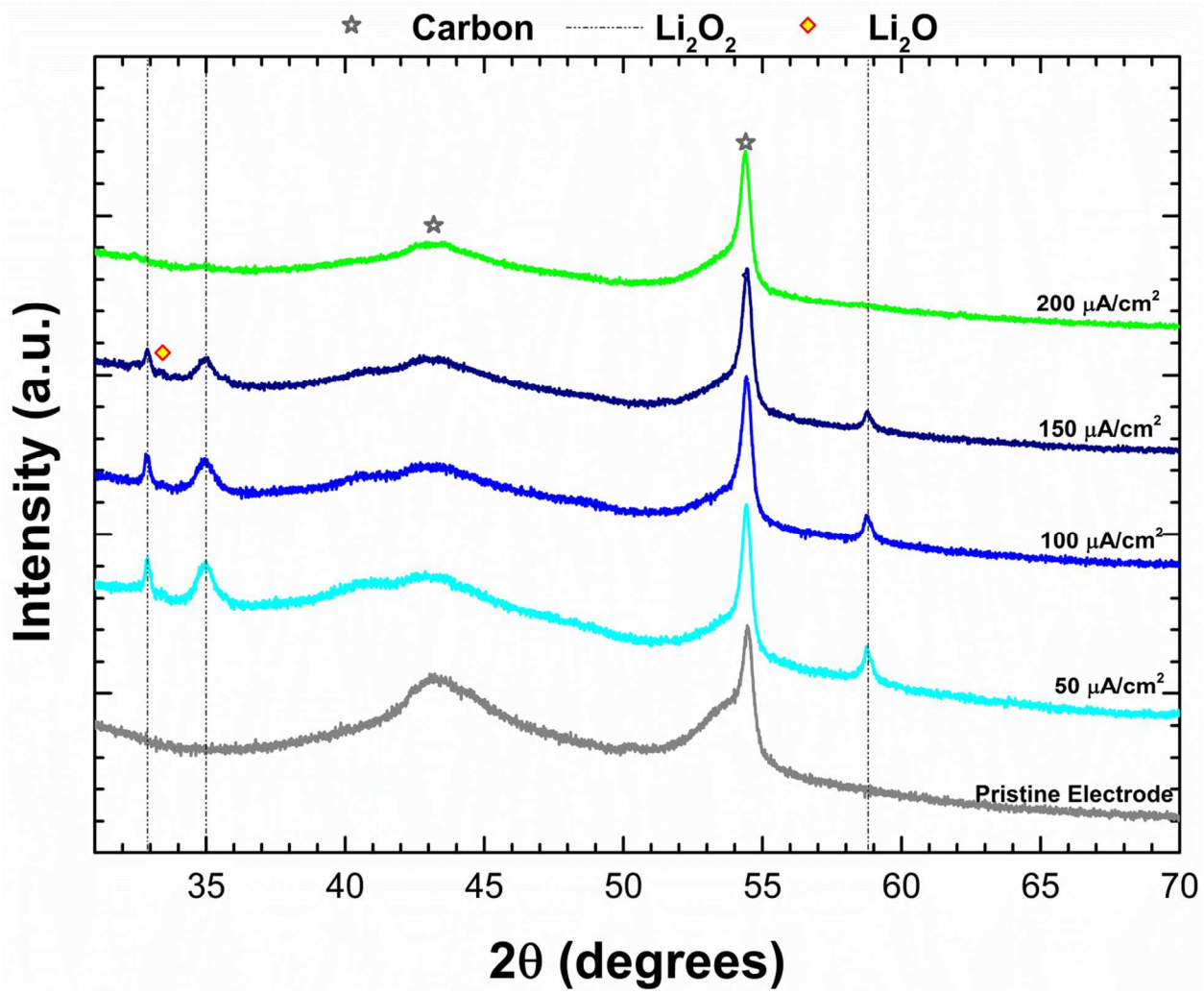

Figure S9 Full XRD patterns of AC electrodes completely discharged at different current densities.

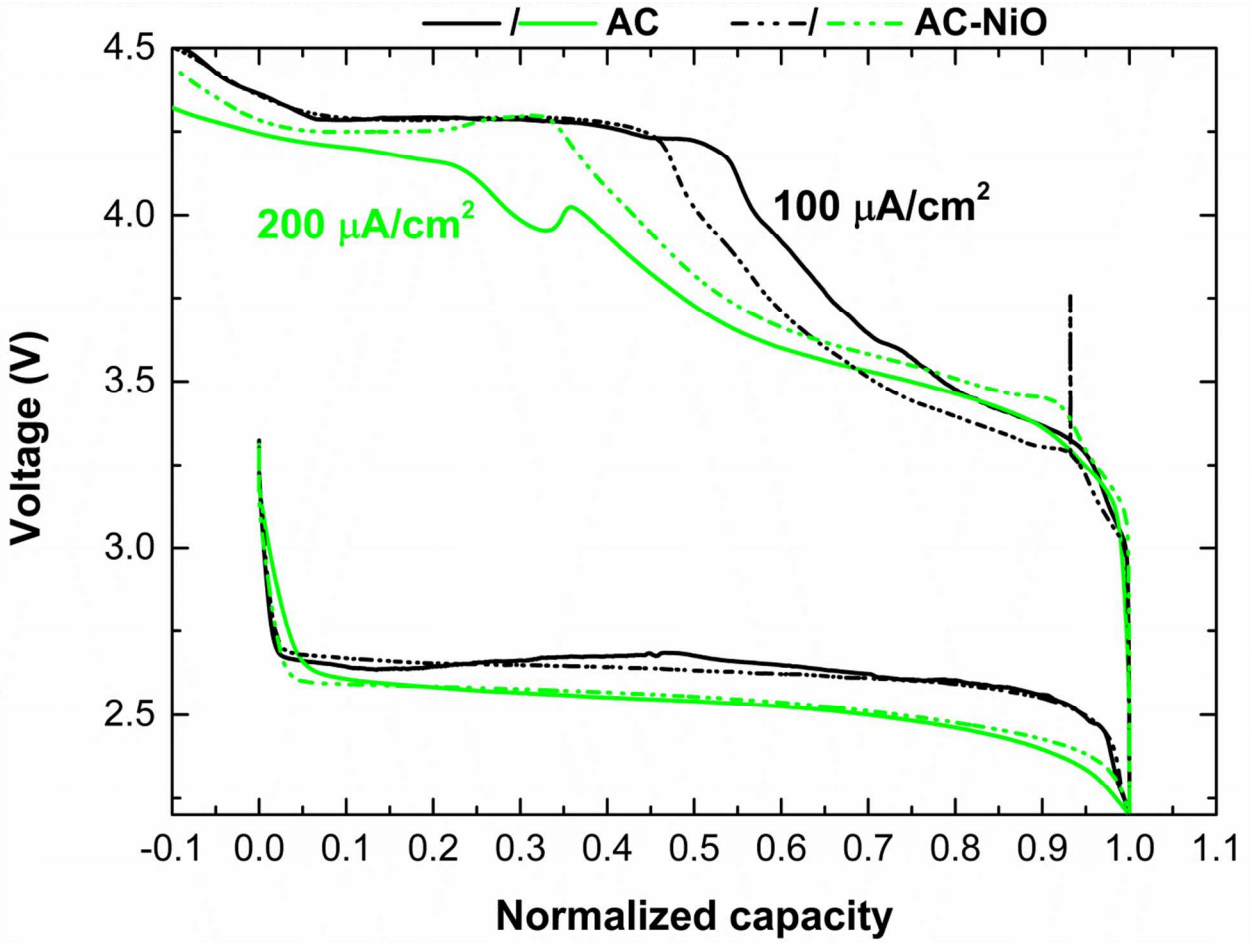

Figure S10 Full galvanostatic (dis)charge profiles of the AC-NiO-1 and AC electrodes in a Li-O_2 cell at current densities of 100 μA/cm^2 and 200 μA/ cm^2 (lower and upper voltage cut-offs set at 2.2 and 4.5 V) with their total capacities normalized to 1.

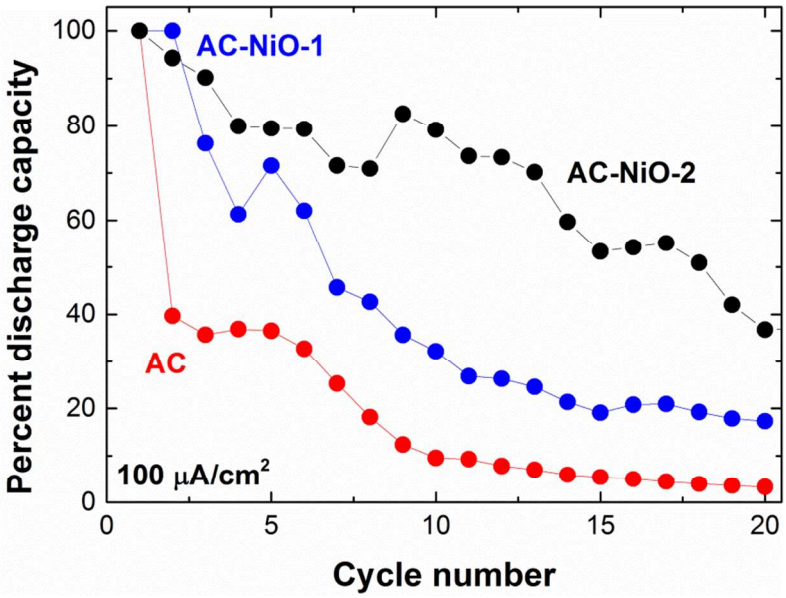

Figure S11 Full and capacity cycling performance of AC-NiO-1/2 and AC electrodes at a current density of 100 μA/cm^2. High and low voltage cutoff of 4.5 V and 2.2 V were set.

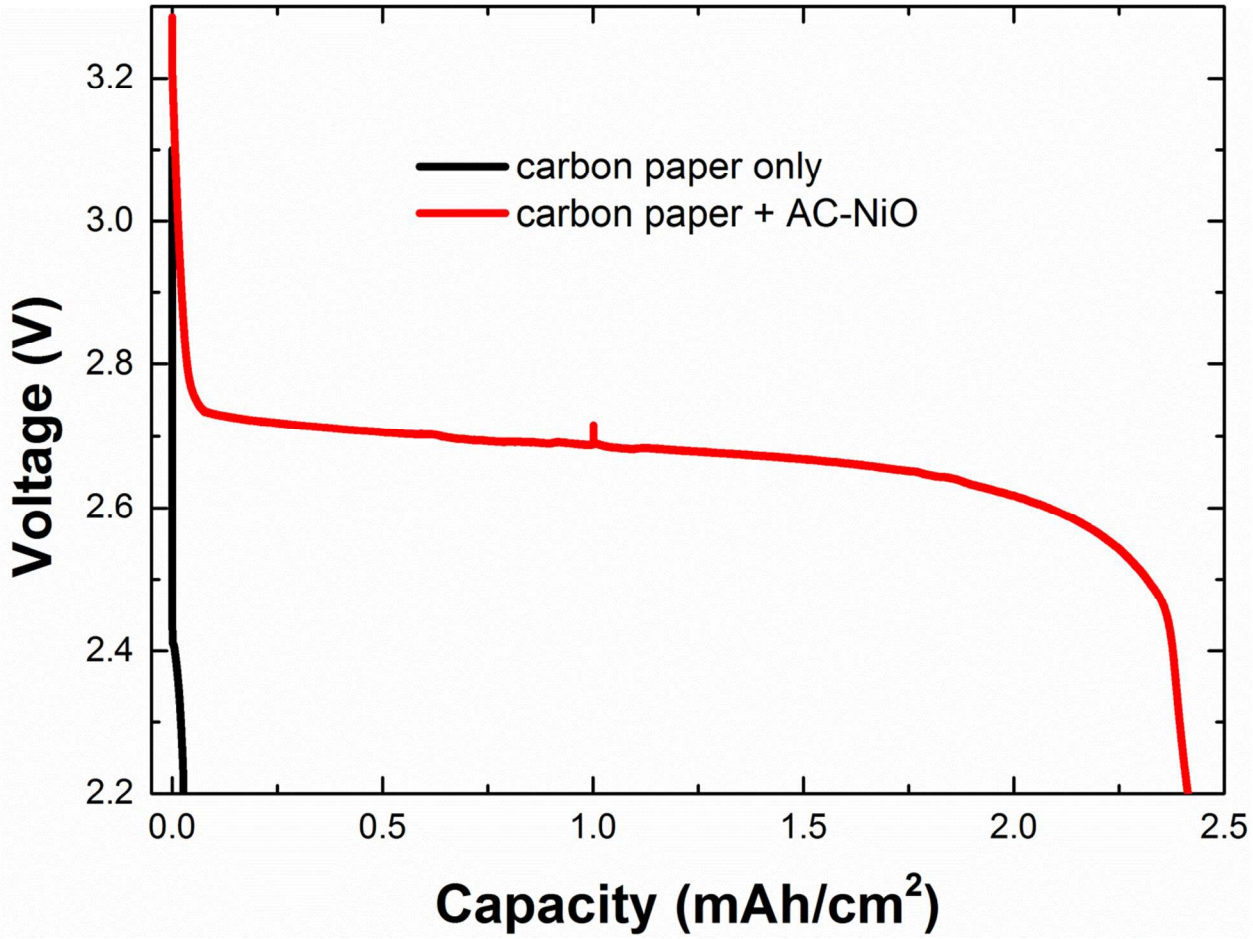

Figure S12 Galvanostatic discharge profiles of carbon paper and carbon paper coated with the AC-NiO mixture at a current density of 50 μA/cm^2 in a Li-O_2 cell.

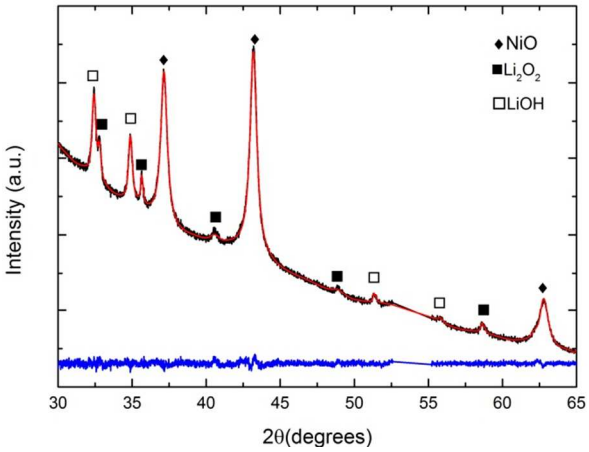

Figure S13 XRD pattern with corresponding Rietveld refinement of AC-NiO-2 electrode after discharge. The black line represents the measured XRD pattern, the red line the fit and the blue line the difference. The different symbols indicate the hexagonal NiO/Li_2O_2 phases.

References

1. A. C. Larson and R. B. Von Dreele, *General Structure Analysis System (GSAS)*, Los Alamos National Laboratory, Los Alamos, NM 87545, 2004.
2. R. R. Garsuch, D. B. Le, A. Garsuch, J. Li, S. Wang, A. Farooq and J. R. Dahn, *J. Electrochem. Soc.*, 2008, **155**, A721-A724.
3. B. D. Adams, C. Radtke, R. Black, M. L. Trudeau, K. Zaghib and L. F. Nazar, *Energy Environ. Sci.*, 2013, **6**, 1772-1778.
4. S. Ganapathy, B. D. Adams, G. Stenou, M. S. Anastasaki, K. Goubitz, X. F. Miao, L. F. Nazar and M. Wagemaker, *J. Am. Chem. Soc.*, 2014, **136**, 16335-16344.
5. J. Heyd, G. E. Scuseria and M. Ernzerhof, *J. Chem. Phys.*, 2003, **118**, 8207-8215.
6. J. Heyd, G. E. Scuseria and M. Ernzerhof, *J. Chem. Phys.*, 2006, **124**.
7. G. Kresse and J. Furthmuller, *Comput. Mater. Sci.*, 1996, **6**, 15.
8. G. Kresse and D. Joubert, *Phys. Rev. B*, 1999, **59**, 1758.
9. S. P. Ong, Y. Mo and G. Ceder, *Phys. Rev. B: Condens. Matter Mater. Phys.*, 2012, **85**.
10. B. D. McCloskey, A. Valery, A. C. Luntz, S. R. Gowda, G. M. Wallraff, J. M. Garcia, T. Mori and L. E. Krupp, *J. Phys. Chem. Lett.*, 2013, **4**, 2989-2993.